IEEE Access
Multidisciplinary | Rapid Review | Open Access Journal

Received June 12, 2019, accepted June 23, 2019, date of publication June 26, 2019, date of current version July 17, 2019.

Digital Object Identifier 10.1109/ACCESS.2019.2925214

An Improved Position-Sensorless Control Method at Low Speed for PMSM Based on High-Frequency Signal Injection into a Rotating Reference Frame

SHUANG WANG, (Member, IEEE), KANG YANG, AND KANG CHEN
School of Mechatronic Engineering and Automation, Shanghai University, Shanghai 200240, China

Corresponding author: Shuang Wang (wang-shuang@shu.edu.cn)

This work was supported in part by the National Key Research & Development Program of China under Grant 2018YFB0104801.

ABSTRACT In this paper, a novel sensorless control strategy with the injection of a high-frequency pulsating sinusoidal voltage into a rotating reference frame for a surface-mounted permanent magnet synchronous motor (SPMSM) is proposed. Conventional schemes may face the problems of applying to the motor with no obvious salient pole effect, and the effect of filter on the bandwidth of the system. Different from the conventional schemes, the new proposed strategy injects a high-frequency pulsating sinusoidal voltage signal is injected into the estimate *d-q* rotating reference frame, and the rotor position information is obtained from the response of injected high-frequency current signal in the α-β stationary reference frame other than the *d-q* rotating reference frame,which can avoid failure of applying to the SPMSM with no obvious salient pole effect. With this approach, band-pass filter, which is necessary in the conventional sensorless control, is removed to simplify the control structure and improve the system dynamic control performance. Therefore, this paper proposes a simple structure, which modulates the high-frequency current signal directly and only passes through the low-pass filter to obtain the estimated rotor position angle. Finally, the feasibility of the improved high-frequency pulsating sinusoidal voltage injection control method is verified by simulation and experiment.

INDEX TERMS Sensorless control, high-frequency pulsating sinusoidal voltage, surface-mounted permanent magnet synchronous motor (SPMSM), salient pole effect.

NOMENCLATURE

PMSM	Permanent magnet synchronous motor
FOC	Field-oriented control
EMF	Electromotive force
HF	High-frequency
SPMSM	Surface-mounted permanent magnet synchronous motor
SNR	Signal-to-noise ratio
EKF	Extended Kalman filter
LPF	Low-pass filter
BPF	Band-pass filter
MRAS	Model reference adaptive system
α-β	Two-phase stationary reference frame
d-q	Two-phase rotating reference frame
$\hat{d}-\hat{q}$	Estimated two-phase rotating reference frame
θ	The actual rotor position angle
$\hat{\theta}$	Estimated rotor position angle
θp	The phase deviation of the fundamental current
$\Delta\theta$	The difference between the actual rotor position angle and the estimated rotor position angle

The associate editor coordinating the review of this manuscript and approving it for publication was Xiaodong Sun.

I. INTRODUCTION

Permanent magnet synchronous motor (PMSM) has become the best choice for many industrial applications because of its high efficiency and high torque density compared with induction machines, especially in the field of advanced manufacturing and electric drive [1]–[5]. As important information of the machine, the rotor position is not only used when the field-oriented control (FOC) scheme is adopted

[6], [7], but also used during calculating the rotor speed for closed loop control. Hence, a mechanical sensor, such as photoelectric encoder and resolver, is usually mounted on the rotor shaft of a PMSM to obtain an accurate rotor position information. However, mechanical position sensors have some problems, such as difficult installation, complex wiring, increasing hardware cost, increasing volume and weight, and easy to fail in special environment such as damp and violent vibration. Hence, in the PMSM control system where the position accuracy is relatively low, such as fans and pumps, the position-sensorless control method is adopted. The advantage of position-sensorless control not only consists in replacing mechanical sensors, but also in providing redundancy protection for the system when the mechanical sensor fails. Therefore, various kinds of sensorless control methods that help to remove mechanical sensor in PMSMs drive systems have been proposed in past decades.

The sensorless control scheme was first proposed by Abbondanti in 1975, since then, it has entered a stage of rapid development [8]–[10]. The sensorless vector control method of PMSM can be divided according to whether the motor is running at middle and high-speed or low speed. The high-speed sensorless method based on the electromotive force (EMF)model to estimate the rotor position works well. In [10], a parallel reduced-order extended Kalman filter (EKF) for rotor position estimation is proposed for the reduction of computation resources. Sliding mode current observer and the adaptive EMF observer designed to estimate the rotor speed and position of PMSM are analyzed in [11]. In [12], the rotor position estimation scheme is achieved by designing a model reference adaptive system (MRAS) observer on the basis of the control winding stator current. In the field of combining artificial intelligence algorithms with motor control, Sun *et al.* [13], [14] proposed the application of neural network algorithm in the field of motor sensorless control. Lin et al. [15] proposed a fuzzy control algorithm to compensate the ideal computed torque controller designed for the tracking of the rotor position reference command. At present, such methods are often combined with other control methods, which is still in the theoretical research stage in the field of motor control because of the complexity of calculation, and there is still a long way to go before practical applications. At very low speed range, however, these position-sensorless control methods couldn't work very well because of the small amplitude of back-EMF signal. To overcome the drawback that the back-EMF is not obvious in the low speed region, usually under 5% of the rated speed, various methods for observing the rotor position based on the salient pole effect or the saturated salient pole effect of the motor have been presented [16],in which, the most popular methods are high-frequency (HF) signal injection methods. The salient-pole tracking method based on high-frequency injection does not depend on the back EMF and motor parameter information, and can achieve better estimation results in the low speed or even zero speed range. According to the types of the injected high-frequency signals, the signal injections can be mainly divided into rotating sinusoidal voltage injection [17], [18], pulsating sinusoidal voltage injection [19], and square-wave voltage injection [20]–[22],and according to the reference frame of the injected high-frequency signals, the injection methods can be mainly divided into two groups: 1) HF voltage injection methods in the stationary α-β reference frame [23]–[25], 2) HF voltage injection methods in the rotary $d-q$ reference frame [26]–[28].

First of all, this paper studies the conventional high-frequency pulsating sinusoidal voltage injection method. The principle of this conventional method is to inject the high-frequency pulsating sinusoidal voltage signal into an axis of the estimated synchronous rotating reference frame, which will interact with rotor-position-dependent saliencies into the machine and modulate the response currents to estimate the rotor position. The information containing the rotor position angle of the motor is extracted from the high-frequency current component. However, in view of the conventional high-frequency pulsating sinusoidal voltage injection method, which relies on the salient pole effect of the motor [29], [30], an improved high-frequency pulsating sinusoidal voltage injection method is proposed, in which, the rotor position angle information is extracted from the high-frequency current response signal in α-β two-phase stationary reference frame, which is independent of the salient polarity of the motor, so it can also be applied to the surface-mounted permanent magnet synchronous motor (SPMSM) with no obvious salient polarity effect. Compared with the conventional method, this method also reduces bandpass filters, which omits the process of extracting high-frequency signals from bandpass filters, demodulates $i_{\alpha h}$ and $i_{\beta h}$ directly, where $i_{\alpha h}$ and $i_{\beta h}$ are the high-frequency current on the α-β two-phase stationary reference frame, respectively, and then filters through low-pass filters to obtain signals containing only the position information of the rotor. This measure simplifies the system structure and eliminates the influence of phase and amplitude of the system caused by bandpass filters, which is one of the main problems to be solved.

This paper is organized as follows: In Section II, the conventional high-frequency pulsating sinusoidal voltage injection method is analyzed. Section III describes the analysis of improved high-frequency pulsating sinusoidal voltage injection method. Experimental results of high-frequency pulsating sinusoidal voltage injection method are presented in Section IV to verify the effectiveness of the proposed sensorless control strategy. Section V summarizes this paper.

II. ANALYSIS OF CONVENTIONAL HIGH-FREQUENCY PULSATING SINUSOIDAL VOLTAGE INJECTION

In the d and q reference frames, the voltage equation of a PMSM can be written as below:

$$\begin{cases} u_d = Ri_d + L_d \dfrac{d}{dt} i_d - \omega_r L_q i_q \\ u_q = Ri_q + L_q \dfrac{d}{dt} i_q + \omega_r L_d i_d + \omega_r \psi_f \end{cases} \tag{1}$$

where $u_d, u_q, i_d, i_q, L_d, L_q$ are the d-q axis stator voltages, d-q axis stator currents, d-q axis inductances, respectively, where R, ω_r, λ_{mpm} are the stator resistances, the rotational speed of the motor, the permanent magnet flux linkage, respectively. This formula represents the actual d-q reference frame and cannot be directly used for position estimation, so it needs to be converted to the estimated position reference frame, or the α-β stationary reference frame. When the PMSM runs at zero or low speed range, the product related to ω_r in formula (1) can be omitted. Therefore, formula (1) can be simplified as below:

$$\begin{cases} u_d = Ri_d + L_d \dfrac{d}{dt} i_d \\ u_q = Ri_q + L_q \dfrac{d}{dt} i_q \end{cases} \tag{2}$$

When the frequency of the injected signal is much larger than the rotational frequency of the motor itself, in this case, the PMSM is equivalent to the pure inductance model [29], so the formula (2) can be written as below:

$$\begin{bmatrix} u_{dh} \\ u_{qh} \end{bmatrix} = \begin{bmatrix} L_{dh} & 0 \\ 0 & L_{qh} \end{bmatrix} P \begin{bmatrix} i_{dh} \\ i_{qh} \end{bmatrix} \tag{3}$$

where u_{dh}, u_{qh}, i_{dh}, i_{qh}, L_{dh}, L_{qh}, P are d-q axis high-frequency voltage, d-q axis high-frequency current, d-q axis high-frequency inductances, derivative operator, respectively.

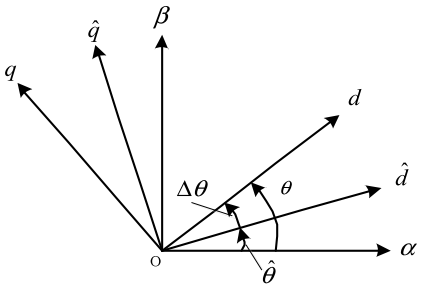

FIGURE 1. Schematic diagram of the angular relationship between the actual reference frame and the estimated reference frame.

The relationship between the estimated $\hat{d} - \hat{q}$ two-phase rotating reference frame and the actual d-q two-phase rotating reference frame is shown in Fig.1. Where θ, $\hat{\theta}$, $\Delta\theta$, are the actual rotor position angle, the estimated rotor position angle, the difference between the actual rotor position angle and the estimated rotor position angle, respectively. As can be seen from Fig.1, the estimated differential response of the current response under the estimated d-q two-phase rotating reference frame can be calculated as below:

$$p \begin{bmatrix} \hat{i}_{dh} \\ \hat{i}_{qh} \end{bmatrix} = T^{-1}(\Delta\theta) p \begin{bmatrix} i_{dh} \\ i_{qh} \end{bmatrix} \tag{4}$$

In the formula, $T(\Delta\theta) = \begin{bmatrix} \cos\Delta\theta & \sin\Delta\theta \\ -\sin\Delta\theta & \cos\Delta\theta \end{bmatrix}$ is the rotation change matrix. The estimated voltage in the d-q two-phase rotating reference frame can be written as:

$$\begin{bmatrix} \hat{u}_{dh} \\ \hat{u}_{qh} \end{bmatrix} = T^{-1}(\Delta\theta) \begin{bmatrix} u_{dh} \\ u_{qh} \end{bmatrix} \tag{5}$$

Substituting (3) into (4), the following can be obtained as:

$$p \begin{bmatrix} \hat{i}_{dh} \\ \hat{i}_{qh} \end{bmatrix} = T^{-1}(\Delta\theta) \begin{bmatrix} \dfrac{1}{L_{dh}} & 0 \\ 0 & \dfrac{1}{L_{qh}} \end{bmatrix} \begin{bmatrix} u_{dh} \\ u_{qh} \end{bmatrix} \tag{6}$$

According to the coordinate axis of the injected high-frequency signal, the injection mode can be divided into two groups: 1) $U_h \cos(\omega_h t)$ is injected from the $\hat{d}$-axis, and then $\hat{i}_q$ is extracted from the $\hat{q}$ -axis for detection. 2) $U_h \cos(\omega_h t)$ is injected from the $\hat{q}$ -axis, and then $\hat{i}_q$ is extracted from the $\hat{d}$ -axis for detection. Where ω_h is the angular frequency of the high-frequency injection signal.

Substituting (5) into (6), the relationship between current and voltage in the estimated $\hat{d} - \hat{q}$ two-phase rotating reference frame can be obtained. If the high-frequency voltage injection axis is chosen on the $\hat{d}$ -axis, the high-frequency current response is:

$$\begin{bmatrix} \hat{i}_{dh} \\ \hat{i}_{qh} \end{bmatrix} = \frac{U_h \sin(\omega_n t)}{\omega_n L_{dh} L_{qi}} \begin{bmatrix} L_{qh}\cos^2\Delta\theta + L_{dh}\sin^2\Delta\theta \\ \dfrac{\sin(2\Delta\theta)}{2}\left(L_{qh} - L_{dh}\right) \end{bmatrix} \tag{7}$$

If the high-frequency voltage injection axis is chosen on the $\hat{q}$ -axis, the high-frequency current response is:

$$\begin{bmatrix} \hat{i}_{dh} \\ \hat{i}_{qh} \end{bmatrix} = \frac{U_h \sin(\omega_h t)}{\omega_h L_{dh} L_{qh}} \begin{bmatrix} \dfrac{\sin(2\Delta\theta)}{2}\left(L_{qh} - L_{dh}\right) \\ L_{qh}\cos^2\Delta\theta + L_{dh}\sin^2\Delta\theta \end{bmatrix} \tag{8}$$

Formula 9 can be obtained from Formula 8 as follows:

$$\hat{i}_{qh} = \frac{U_h\left(L_{qh} - L_{dh}\right)}{2\omega_h L_{dh} L_{qh}} \sin(\omega_h t)\sin(2\Delta\theta) \tag{9}$$

Ideally, when the PMSM rotor position estimation system enters the steady state, the estimated value of the position is consistent with the actual value. At this time, the position estimation error $\Delta\theta = 0$. It can be seen from formula (7) and formula (8) that the high-frequency current response $\hat{i}_{qh}$ produced by injecting high-frequency voltage into $\hat{d}$ -axis is equal to 0 in the steady state of the system, which has no effect on the system torque; while the high-frequency current response $\hat{i}_{qh}$ produced by injecting high-frequency voltage into $\hat{q}$ -axis is not equal to 0 in the steady state of the system, and a large torque ripple is generated to cause the motor to shake, thereby affecting the estimation accuracy of the rotor position. Therefore, $\hat{d}$ -axis signal injection is used in this chapter. The rotor position estimation error $\Delta\theta$ can be obtained by detecting the $\hat{q}$ -axis current and performing appropriate processing on the current signal. After the multiplier and low pass filter (LPF), the output current containing the error of rotor position estimation can be obtained as:

$$LPF\left(\hat{i}_{qh} \times \sin(\omega_h t)\right) = k\sin(2\Delta\theta) \tag{10}$$

where

$$k = \frac{U_h\left(L_{qh} - L_{dh}\right)}{4\omega_h L_{dh} L_{qh}} \tag{11}$$

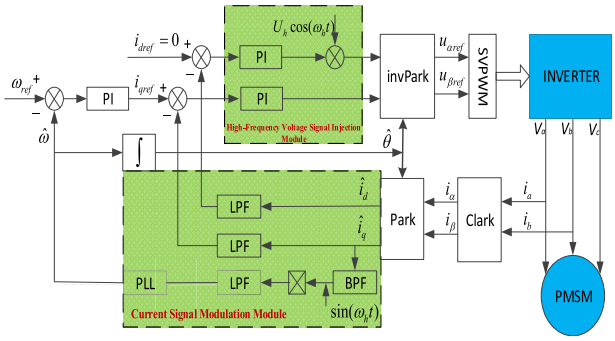

FIGURE 2. Structural block diagram of conventional high-frequency pulsating sinusoidal voltage injection method.

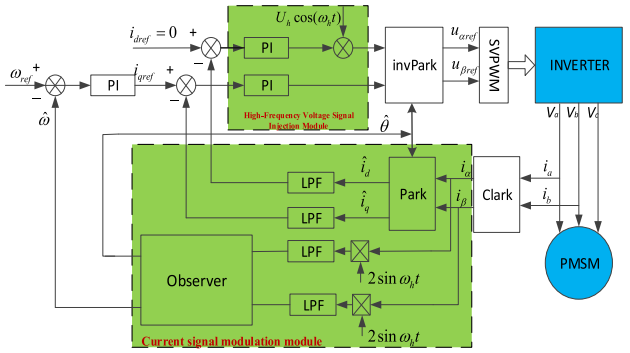

FIGURE 3. Structural block diagram of improved high-frequency pulsating sinusoidal voltage injection method.

It can be seen that the estimated rotor position can be equal to the actual rotor position by adjusting the formula (9) to zero through appropriate control method. The specific implementation block diagram is shown in Figure 2.

III. ANALYSIS OF IMPROVRD HIGH-FREQUENCY PULSATING SINUSOIDAL VOLTAGE INJECTION

Although the conventional high-frequency pulsating sinusoidal voltage injection method can effectively extract the rotor position information and get the estimated rotor position, the method depends on the saliency of the motor structure or saturation saliency. Once the saliency is not obvious, the signal-to-noise ratio (SNR) of position-related signals is very small, which is one of the main problems to be solved. It is difficult to extract the angle signal, which results in the failure of rotor position estimation [31].

It can be seen from formula (9) that when the salient pole effect of SPMSM is not obvious, L_{dh} and L_{qh} are approximately equal. At this time, L_{qh} minus L_{dh} is equal to 0, and formula (8) is equal to 0. The position estimation error information will be small, and it is difficult to extract the angle signal, which will cause the angle estimation to fail. At the same time, the use of the bandpass filter in Figure 2 affects the phase and amplitude of the system signal. To solve these problems, an improved high-frequency pulsating sinusoidal voltage injection method is proposed in this paper. This method does not depend on the salient polarity of the motor, and the effect of the bandpass filter on the signal is reduced, which can better observe the rotor position of PMSM. The detailed analysis is as follows.

A. ROTOR POSITION EXTRACTION

The high-frequency pulsating sinusoidal voltage is injected into the $\hat{d}$ -axis of the estimated rotating reference frame, and the angle signal is extracted from the high-frequency current response of the α-β two-phase stationary reference frame. The specific control block diagram is shown in Figure 3.

Formula (3) is the high-frequency voltage equation of the d-q reference frame of the PMSM under high-frequency signal injection. The current of d-q axis in formula (3) can be converted to the current of α-β axis, which can be equivalent to the following formula:

$$\begin{bmatrix} u_{dh} \\ u_{qh} \end{bmatrix} = \begin{bmatrix} L_{dh} & 0 \\ 0 & L_{qh} \end{bmatrix} T(\theta) P \begin{bmatrix} i_{\alpha h} \\ i_{\beta h} \end{bmatrix} \tag{12}$$

where

$$T(\theta) = \begin{bmatrix} \cos\theta & \sin\theta \\ -\sin\theta & \cos\theta \end{bmatrix} \tag{13}$$

The high-frequency current response of PMSM in α-β two-phase stationary reference frame can be derived from formula (12):

$$P \begin{bmatrix} i_{\alpha h} \\ i_{\beta h} \end{bmatrix} = T^{-1}(\theta) \begin{bmatrix} \frac{1}{L_{di}} & 0 \\ 0 & \frac{1}{L_{qh}} \end{bmatrix} \begin{bmatrix} u_{dh} \\ u_{qh} \end{bmatrix} \tag{14}$$

Substituting (5) into (14), the formula (15) can be obtained as shown in bottom of this page. Inject a high-frequency pulsating sinusoidal voltage signal into the $\hat{d}$ -axis of the estimated rotating reference frame:

$$\begin{bmatrix} \hat{u}_{dh} \\ \hat{u}_{qh} \end{bmatrix} = \begin{bmatrix} U_h \cos\omega_h t \\ 0 \end{bmatrix} \tag{16}$$

$$P \begin{bmatrix} i_{\alpha h} \\ i_{\beta h} \end{bmatrix} = \begin{bmatrix} \frac{1}{L_{d\mathrm{h}}} \cos\theta\cos\Delta\theta + \frac{1}{L_{qh}} \sin\theta\sin\Delta\theta & \frac{1}{L_{dh}} \cos\theta\sin\Delta\theta - \frac{1}{L_{qh}} \sin\theta\cos\Delta\theta \\ \frac{1}{L_{dh}} \sin\theta\cos\Delta\theta - \frac{1}{L_{qh}} \cos\theta\sin\Delta\theta & \frac{1}{L_{dh}} \sin\theta\sin\Delta\theta + \frac{1}{L_{qh}} \cos\theta\cos\Delta\theta \end{bmatrix} \begin{bmatrix} \hat{u}_{dh} \\ \hat{u}_{qh} \end{bmatrix} \tag{15}$$

Substituting (16) into (15), the formula (17) can be obtained as:

$$\begin{bmatrix} i_{ah} \\ i_{\beta h} \end{bmatrix} = \frac{U_h}{\omega_h} \begin{bmatrix} \frac{1}{L_{di}} \cos\theta \cos\Delta\theta + \frac{1}{L_{qh}} \sin\theta \sin\Delta\theta \\ \frac{1}{L_{di}} \sin\theta \cos\Delta\theta - \frac{1}{L_{qi}} \cos\theta \sin\Delta\theta \end{bmatrix} \sin\omega_h t \tag{17}$$

It can be seen from formula (17) that the high-frequency current response in α-β two-phase stationary reference frame contains rotor position information. If the angular error $\Delta\theta$ is small enough, the estimated rotor position converges to the actual rotor position. L_{dh} is equal to L_{qh} for a SPMSM, so the stationary α-β two-phase high-frequency current response can be simplified as follows:

$$\begin{bmatrix} i_{ah} \\ i_{\beta h} \end{bmatrix} = \frac{U_h}{\omega_h L_{dh}} \begin{bmatrix} \cos\theta \\ \sin\theta \end{bmatrix} \sin\omega_h t \tag{18}$$

In position-sensorless control using high-frequency pulsating sinusoidal voltage injection method, the current vector $i_{\alpha\beta}$ in two-phase stationary reference frame includes the fundamental current vector $i_{\alpha\beta b}$, the high-frequency current component $i_{\alpha\beta h}$, and the high order harmonic current vector $i_{\alpha\beta x}$ caused by the PWM switching signal.

$$\boldsymbol{i_{\alpha\beta} = i_{\alpha\beta b} + i_{\alpha\beta h} + i_{\alpha\beta x}} \tag{19}$$

In the formula (19), $i_{\alpha\beta h}$ contains the position information of the rotor. Generally, it is necessary to extract the high-frequency current component $i_{\alpha\beta h}$ with a band-pass filter. However, the use of the band-pass filter will increase the complexity of the system. More seriously, it will cause the shift of the amplitude and phase of the signal [32], which affects the accuracy of the estimation. For example, the high-frequency signal with 900Hz frequency is extracted by bandpass filter. The type of bandpass filter is Butterworth, the order is 4, the low-pass cut-off frequency is 600 Hz, and the high-pass cut-off frequency is 1200 Hz. The phase-frequency characteristic curve of the band-pass filter designed according to the above requirements is shown in Figure 4.

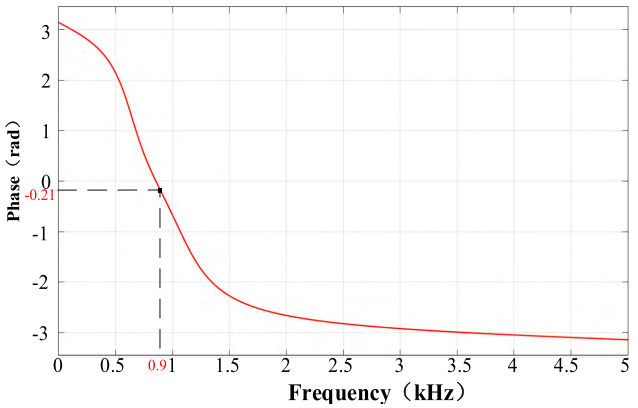

FIGURE 4. Phase-frequency characteristic curve of bandpass filter.

From the phase-frequency characteristic curve, it can be seen that a high-frequency signal passing through the band-pass filter produces a phase shift of 0.21 rad at 900 Hz. This phase shift also changes as the order of the filter, the cut-off frequency, the passband bandwidth, and the frequency of the injected high frequency signal change. Therefore, the use of a bandpass filter causes a phase shift in the signal and a bias in the estimated angle, which is one of the main problems to be solved below.

Document [33], [34] analyses the angle estimation error caused by bandpass filter, and proposes a phase compensation algorithm, which improves the angle error effectively. However, additional compensation algorithm needs to add a large number of calculation modules, which further increases the complexity of the system.

In order to solve the signal phase shift problem caused by the band-pass filter, this paper adopts the method that the static two-phase current $i_{\alpha h}$ and $i\beta h$ have modulated directly. Only the low-pass filter is required to obtain the signal containing the rotor position information, and the band-pass filter is omitted, which simplifies the system structure and eliminates the effects of bandpass filters on signal amplitude and phase. The structure diagrams before and after simplification are shown in Figure 5.

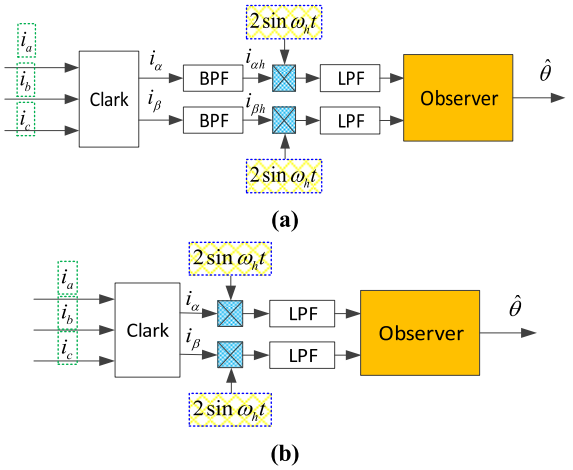

FIGURE 5. Structural chart of rotor position estimation. (a) Before simplification. (b) After simplification.

During the operation of PMSM at low speed, the fundamental current $i_{\alpha\beta b}$ is multiplied by the modulation signal $2\,sin\omega_h t$, and the following formula can be obtained as:

$$\begin{aligned} & i_{\alpha\beta b} \times 2\sin\omega_h t \\ &= \begin{bmatrix} i_{\alpha b} \\ i_{\beta b} \end{bmatrix} 2\sin\omega_h t \\ &= 2\,k \begin{bmatrix} \cos\omega_r t - \theta_p \\ \sin\omega_r t - \theta_p \end{bmatrix} \sin\omega_h t \\ &= k \begin{bmatrix} \sin(\omega_r + \omega_h)\,t + \sin(\omega_h - \omega_r)\,t - 2\theta_p \sin\omega_h t \\ \cos(\omega_r + \omega_h)\,t - \cos(\omega_h - \omega_r)\,t - 2\theta_p \sin\omega_h t \end{bmatrix} \end{aligned} \tag{20}$$

where k is the amplitude of the fundamental current, ω_r is the rotational angular frequency of the motor, and $\boldsymbol{\theta}_p$ is the phase deviation of the fundamental current.

Since the rotational frequency of the fundamental current ω_r at low speed is very low and much smaller than ω_h, it can be seen from formula (20) that the signal obtained by multiplying $i_{\alpha\beta b}$ and $2sin\omega_h t$ is composed of three high-frequency signals, so the signal can be filtered by low-pass filter. Similarly, the frequency of high-order harmonic current $i_{\alpha\beta x}$ is much higher than the frequency of injection signal, and the signal multiplied by $2sin\omega_h t$ is still high-frequency harmonic signal, which can also be filtered by low-pass filter. Hence, it can be concluded that:

$$\begin{aligned}\begin{bmatrix} i_{\alpha l} \\ i_{\beta l} \end{bmatrix} &= LPF\left(\begin{bmatrix} i_{\alpha} \\ i_{\beta} \end{bmatrix} 2\sin\omega_h t\right) \\ &= LPF\left(\begin{bmatrix} i_{\alpha h} \\ i_{\beta h} \end{bmatrix} 2\sin\omega_h t\right) \\ &= \frac{U_h}{\omega_h L_{dh}} \begin{bmatrix} \cos\theta \\ \sin\theta \end{bmatrix} \end{aligned} \tag{21}$$

It can be seen from formula (21) that the improved high-frequency pulse voltage injection method is only related to the inductance value and does not depend on the salient polarity of PMSM, so it is suitable for SPMSM with very small salient polarity. The actual rotor position information can be obtained by processing the high-frequency current signal. The results obtained by using $i_{\alpha\beta}$ directly multiplied by $2sin\omega_h t$ and filtering by low-pass filter are consistent with those obtained by using $i_{\alpha\beta h}$ modulation and filtering by low-pass filter. In the process of processing, the band-pass filter is omitted, the amplitude attenuation and phase shift caused by the band-pass filter are eliminated, and the system structure is simplified. Therefore, the improved method proposed in this paper solves the two drawbacks of the conventional high-frequency pulsating sinusoidal voltage injection method.

B. ROTOR POSITION OBSERVER

In this paper, the two-phase phase-locked loop observer is used to observe the rotor position and rotational speed. The specific structure is shown in Figure 6.

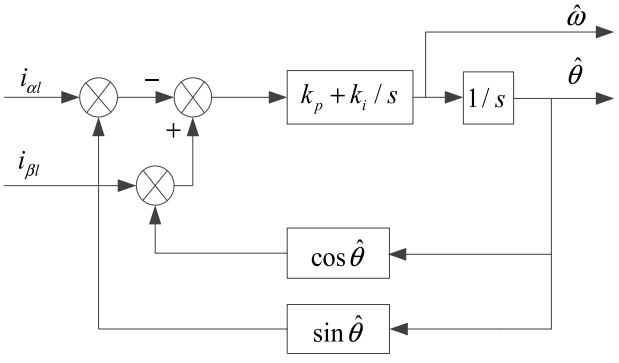

FIGURE 6. Two-phase phase-locked loop structure block diagram.

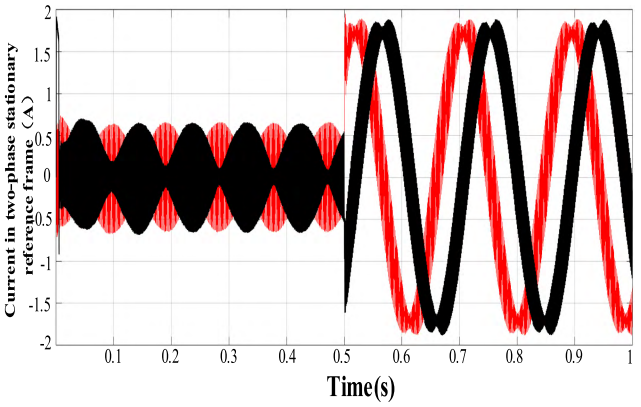

FIGURE 7. Current waveform in two-phase stationary reference frame.

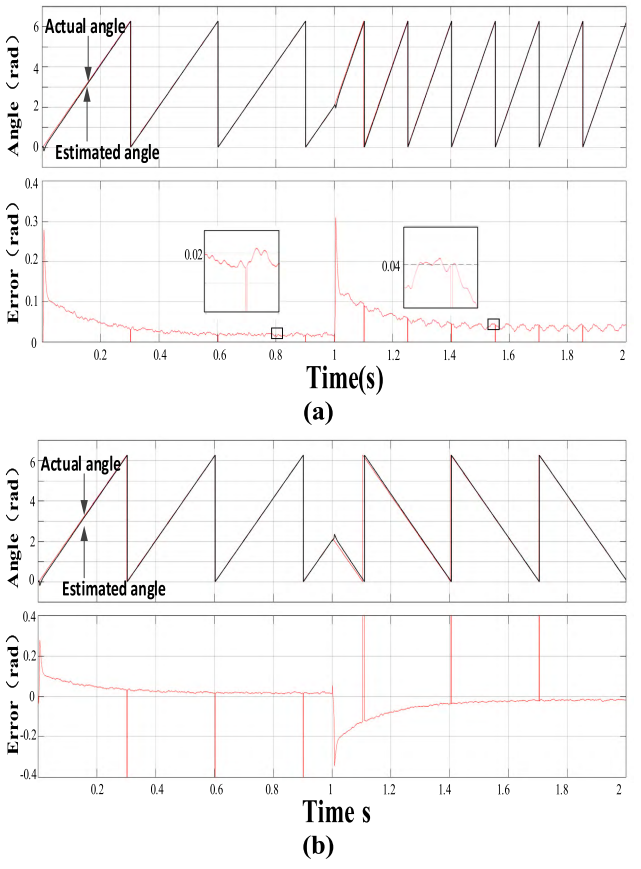

FIGURE 8. Dynamic performance of conventional high-frequency pulsating sinusoidal voltage injection method. (a) Estimated angle waveform at sudden change of speed. (b) Estimated angle waveform for steering abrupt change.

From Fig.6, the rotor position error signal for observation can be obtained as follows:

$$\varepsilon = i_{\beta l}\cos\hat{\theta} - i_{\alpha l}\sin\hat{\theta} = k_h \sin(\theta - \hat{\theta}) \tag{22}$$

where

$$k_h = \frac{U_h}{\omega_h L_{dh}}$$

When the angle error between estimated angle and actual angle $\boldsymbol{\theta} - \hat{\boldsymbol{\theta}}$ is very small, formula (22) can be simplified

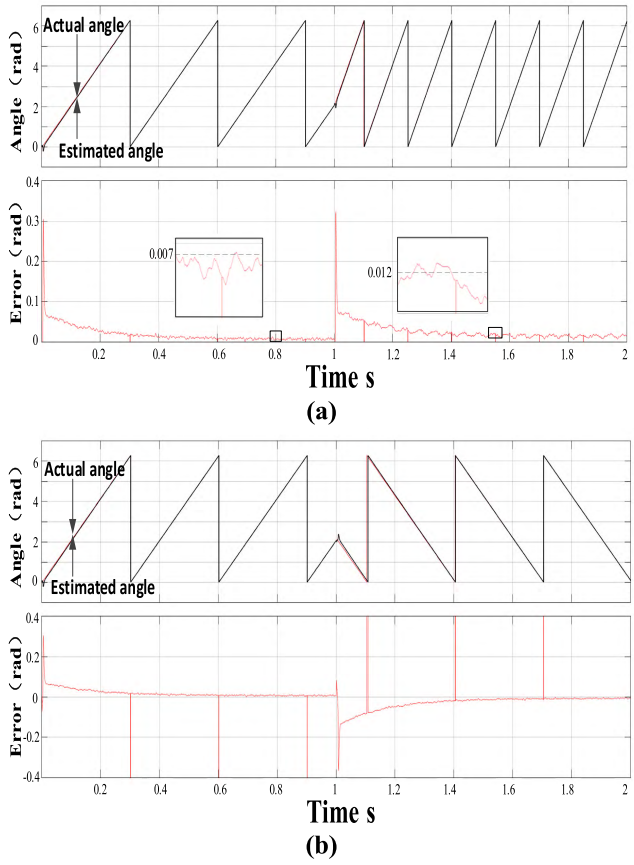

FIGURE 9. Dynamic performance of improved high-frequency pulsating sinusoidal voltage injection method (a) Estimated angle waveform at sudden change of speed. (b) Estimated angle waveform for steering abrupt change.

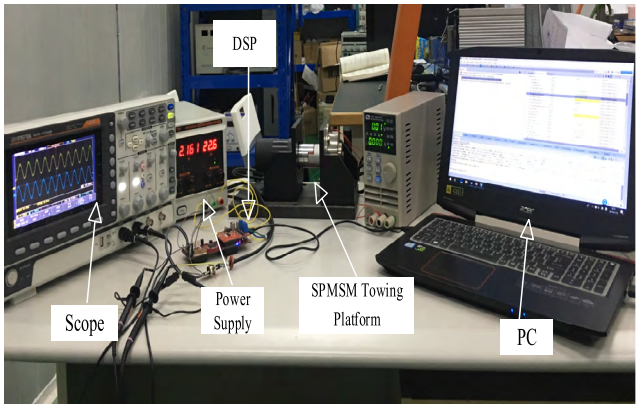

FIGURE 10. Test bench description.

as follows:

$$\varepsilon = k_h \sin(\theta - \hat{\theta}) \approx k_h(\theta - \hat{\theta}) \tag{23}$$

Therefore, the closed-loop transfer function of the two-phase phase-locked loop can be expressed as:

$$\frac{\hat{\theta}}{\theta} = \frac{k_h k_p s + k_h k_i}{s^2 + k_h k_p s + k_h k_i} \tag{24}$$

Since k_h is a positive number, it can be judged from Rolls-Holwitz theorem that the system is stable when $k_h k_p$ and

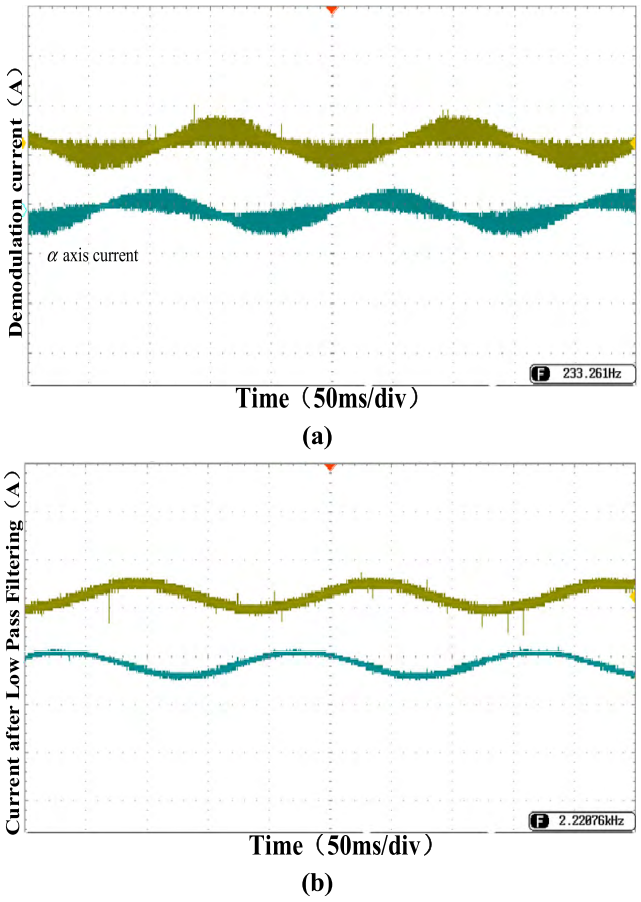

FIGURE 11. Current signal processing (a)Waveform after modulation of high-frequency current signal(b)Output waveform of low-pass filter.

$k_h k_i$ are both positive numbers. Therefore, PLL can lock the angle well and the estimated rotor position can converge to the actual rotor position.

C. SIMULATION RESULTS

The feasibility of the improved high-frequency pulsating sinusoidal voltage injection method has been verified by theoretical analysis. Due to the complexity of the control system, simple theoretical analysis is difficult to function in system analysis and design, so it is necessary to carry out auxiliary verification through computer simulation research. In this paper, the conventional high-frequency pulsating sinusoidal voltage injection method and the improved high-frequency pulsating sinusoidal voltage injection method for PMSM rotor position estimation model are built on MATLAB/Simulink simulation platform to verify the correctness of theoretical derivation. The simulation parameters of the motor body in this paper are derived from a SPMSM used in the experiment. The rated voltage and the rated current are set to 24V, and 4.6A, respectively, in the simulations. The rated power of the motor, the pole pair, the stator resistance and the cross-axis inductance are set to 70W, 2 pairs, 0.27Ω, and 0.9mH, respectively.

The vector control strategy of $i_d = 0$ is adopted in the simulation to realize the position sensorless control of the

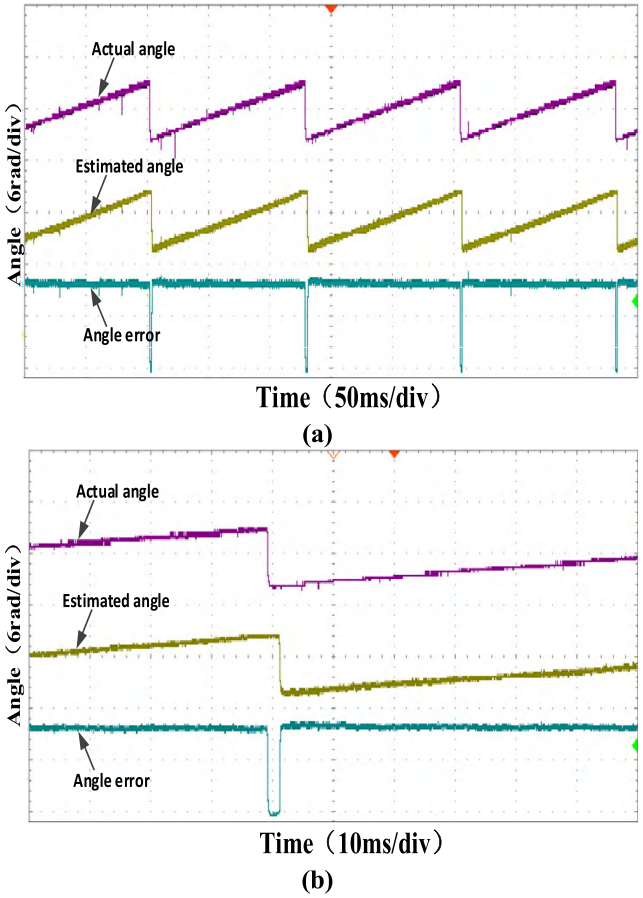

FIGURE 12. Conventional high-frequency pulsating sinusoidal voltage injection method for rotor position observation at 100rpm. (a) Angle comparison. (b) Angle contrast magnification.

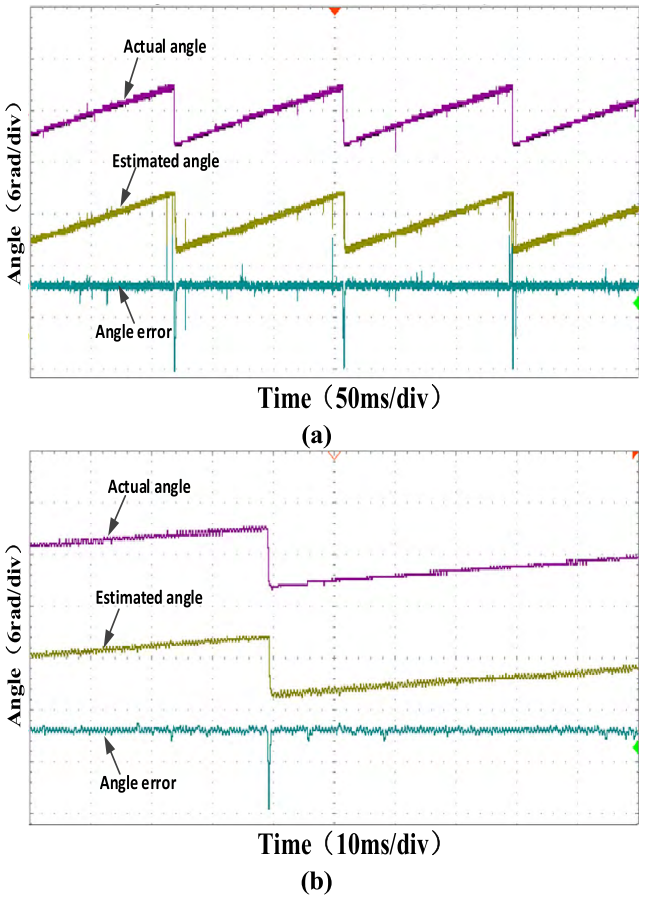

FIGURE 13. Improved high-frequency pulsating sinusoidal voltage injection method for rotor position observation at 100rpm. (a) Angle comparison. (b) Angle contrast magnification.

low speed range of the PMSM. A high-frequency pulsating sinusoidal voltage signal having a frequency of 900 Hz and an amplitude of 5 V is injected on the estimated d-axis, and rotor position information is extracted from the high-frequency current response of the two-phase stationary reference frame. In the conventional high-frequency pulsating sinusoidal voltage injection method, the high-pass cut-off frequency of the band-pass filter for extracting the high-frequency current signal is set to 1200 Hz, and the low-pass cut-off frequency is set to 600 Hz, which ensures efficient extraction of the high-frequency current response signal.

The amplitude of the high-frequency sinusoidal signal used for modulation is 2V and the frequency is 900 Hz. The cut-off frequency of the low-pass filter for extracting the modulated signal is set to 300 Hz. Finally, the angular and velocity signals are solved by using a two-phase phase phase-locked loop. The position estimator of the improved high-frequency pulsating sinusoidal voltage injection method omits the band-pass filter on the basis of the original model and directly modulates the current signal. Figure 7 is the current waveform in two-phase stationary reference frame and the current harmonic content in Figure 7 is mainly caused by high-frequency injection voltage. It can be seen from Figure 7 that the two-phase current has good sinusoidal characteristics when the load is suddenly applied for 0.5 seconds.

Figure 8 shows the simulation waveform of the dynamic performance of the conventional high-frequency pulsating sinusoidal voltage injection method. Fig.8(a) is the contrast waveform between the actual angle and the estimated angle when the motor speed changes suddenly. The motor suddenly accelerates from 50 rpm to 100 rpm in 1 second, and the angular error is about 0.3 rad. In the steady state, the estimated error of 100 rpm is about 0.04 rad, and the estimated error of 50 rpm is about 0.02 rad less than 100 rpm. It can be seen that the estimation accuracy of high-frequency pulsating sinusoidal voltage injection method is related to the speed, and the smaller the speed, the higher the estimation accuracy. Fig.8(b) shows that the PMSM suddenly changes from 50 rpm to −50 rpm in 1 second. It can be seen from the figure that when the motor is switched from forward to reverse, the angle estimation will fluctuate slightly. The angle error is less than 0.4 rad, and the estimated angle basically follows the actual angle.

Figure 8. Dynamic performance of conventional high-frequency pulsating sinusoidal voltage injection method (a) Estimated angle waveform at sudden change of speed. (b) Estimated angle waveform for steering abrupt change.

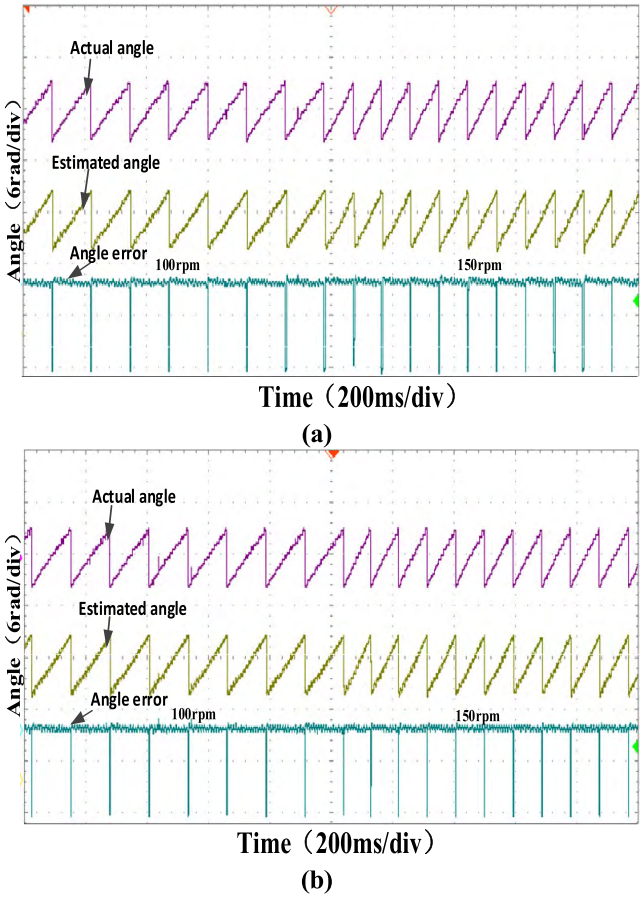

FIGURE 14. Rotor position observation at sudden change of speed. (a) Conventional high-frequency pulsating sinusoidal voltage injection method. (b) Improved high-frequency pulsating sinusoidal voltage injection method.

Figure 9 shows the simulation waveform of the dynamic performance of the improved high-frequency pulsating sinusoidal voltage injection method. Fig.9(a) shows the simulation waveform of the motor speed from 50 rpm to 100 rpm in 1 second. It can be seen that the estimated angle can converge to the actual angle faster than previous one, and the estimation accuracy is higher. Fig.9(b) is a simulation waveform of the sudden change of the motor speed from 50 rpm to −50 rpm in 1 second. It can be seen that the angle estimation will produce small fluctuations when the motor is switched from forward to reverse. Compared with the conventional high-frequency pulsating sinusoidal voltage injection method, the estimated angle can follow the actual angle faster and the phase delay is smaller. It can be seen that the improved high-frequency pulsating sinusoidal voltage injection method can effectively eliminate the phase shift problem caused by the band-pass filter, and the injection method has higher estimation accuracy and better dynamic performance.

IV. EXPERERIMENTAL RESULTS

The proposed sensorless control scheme was verified on the platform with a 70W SPMSM, as shown in Fig. 10. The system mainly involves the upper computer PC that sends the command and monitors the system status, the SPMSM tow platform, the oscilloscope and the control system and the drive system of DSP. The controlled motor and the magnetic powder brake are connected by a coupling. The main electrical parameters of the SPMSM are shown in Table 1.

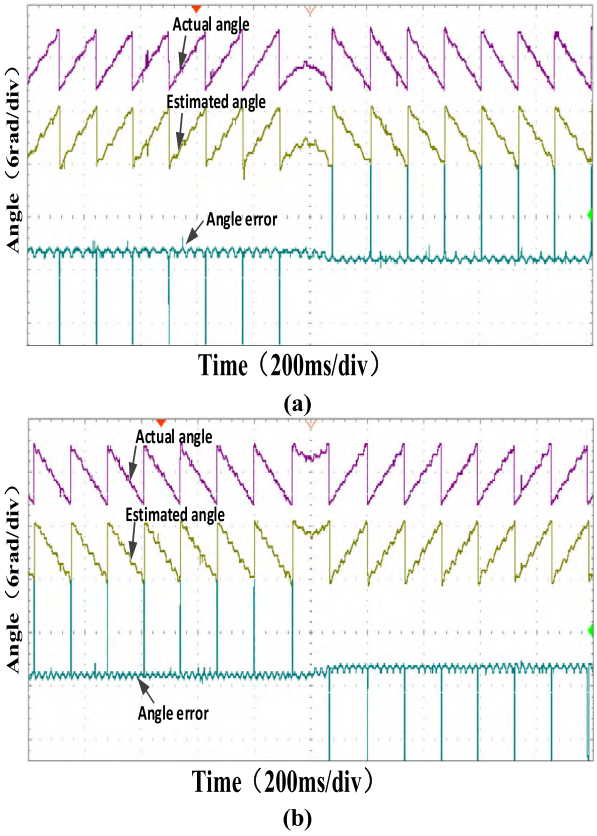

FIGURE 15. Conventional high-frequency pulsating sinusoidal voltage injection method for rotor position observation during steering abrupt change. (a) Steering of motor from forward to reverse. (b) Steering of motor from reverse to forward.

TABLE 1. Motor parameters.

Parameter	Value
Stator Resistance /Ω	0.27
d-axis Inductance /H	0.0009
q-axis Inductance /H	0.0009
Flux Linkage /Wb	0.098
Pole Number	2
Rated Voltage /V	24
Rated Current /A	4.6
Rated Speed /rpm	3000
Rated Torque /N·m	0.32

A. IMPROVED HIGH-FREQUENCY PULSATING SINUSOIDAL VOLTAGE INJECTION METHOD FOR CURRENT SIGNAL PROCESSING

In the improved experimental method, the interruption frequency of the system is set as 10 kHz. In the cases of rotor position estimation, the magnitude of the injection sinusoidal signal voltage is 10 V, and its frequency is 1000 Hz. The given motor speed instruction is 100 rpm, and the motor runs from start-up to stable state under no-load condition. Fig.11(a) is

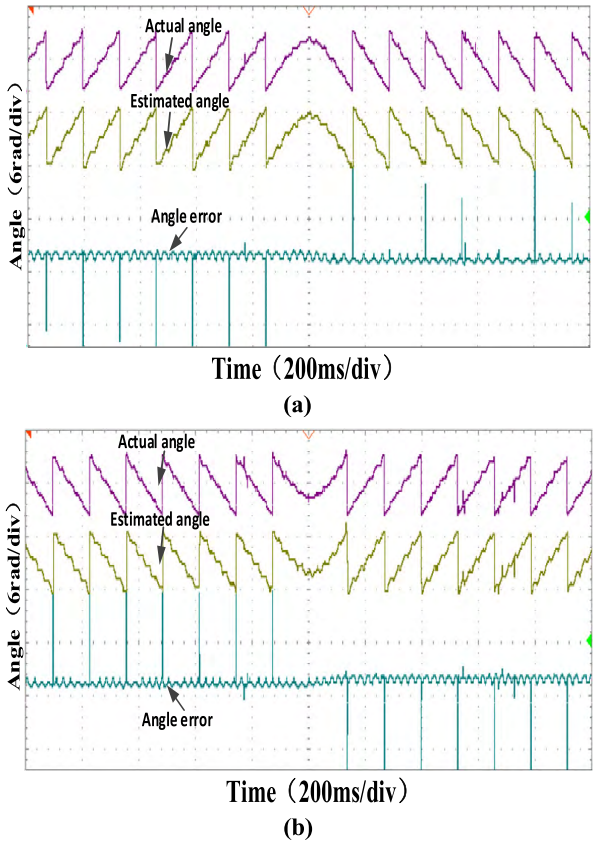

FIGURE 16. Improved high-frequency pulsating sinusoidal voltage injection method for rotor position observation during steering abrupt change. (a) Steering of motor from forward to reverse. (b) Steering of motor from reverse to forward.

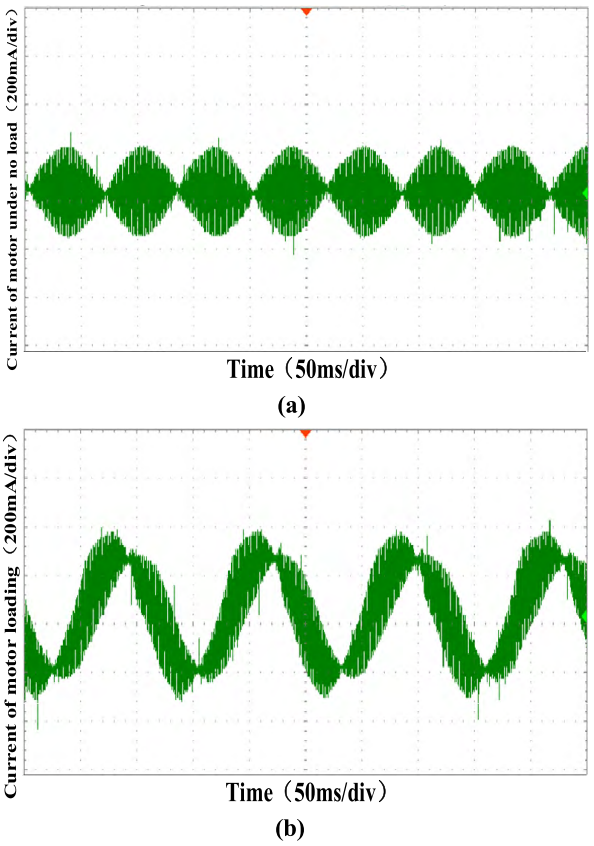

FIGURE 17. Phase current waveform of high-frequency pulsating sinusoidal voltage injection method. (a)Phase current waveform of motor under no load. (b) Phase current waveform of motor loading.

a waveform obtained by modulating the current $i_{\alpha\beta h}$. The waveform in Fig.11(a) passes through a digital low-pass filter and outputs the waveform in Fig.11(b). The rotor angle signal of the motor can be observed after the waveform of Fig.11(b) passes through the observer.

From the experimental waveforms, it can be seen that the digital low-pass filter designed in the experiment can effectively obtain the sinusoidal wave signal containing the position information of the rotor.

B. OBSERVATION EXPERIMENT OF MOTOR ROTOR POSITION AT 100RPM OPERATION

Given the motor speed of 100 rpm, Fig.12 is the experimental waveform of rotor position observation based on conventional high-frequency pulsating sinusoidal voltage injection method and Fig.13 is the experimental waveform of rotor position observation based on improved high-frequency pulsating sinusoidal voltage injection method.

The experimental waveforms show that the two high-frequency injection methods can effectively observe the rotor position. The steady-state error between the estimated angle and the actual angle of the conventional high-frequency pulsating sinusoidal voltage injection method is about 0.12 rad, and the phase delay is about 0.06 rad. The steady-state error between the estimated angle and the actual angle of the improved high-frequency pulsating sinusoidal voltage injection method is about 0.08 rad, and the phase delay is about 0.03 rad. The improved method eliminates the influence of band-pass filter on angle estimation performance, improves the estimation accuracy and reduces the phase delay of angle estimation, so it has better steady-state performance.

C. OBSERVATION EXPERIMENT OF ROTOR POSITION OF MOTOR IN SUDDEN CHANGE OF SPEED

Fig.14 is the experimental waveform of rotor position observation in case of sudden change of speed. Among them, Fig.14(a) is the rotor position observation waveforms obtained by using the conventional high-frequency pulsating sinusoidal voltage injection method. Fig.14(b) is the rotor position observation waveforms obtained by using the improved high frequency pulse voltage injection method.

From the experimental waveforms, it can be seen that the two high-frequency injection position estimation methods can effectively observe the rotor position information in case of sudden change of rotational speed. The phase delay of the improved high-frequency pulse voltage injection method is about 0.05 rad, which is obviously reduced compared with the angle phase delay of 0.1 rad before improvement. The observation effect is better than the previous angle observation.

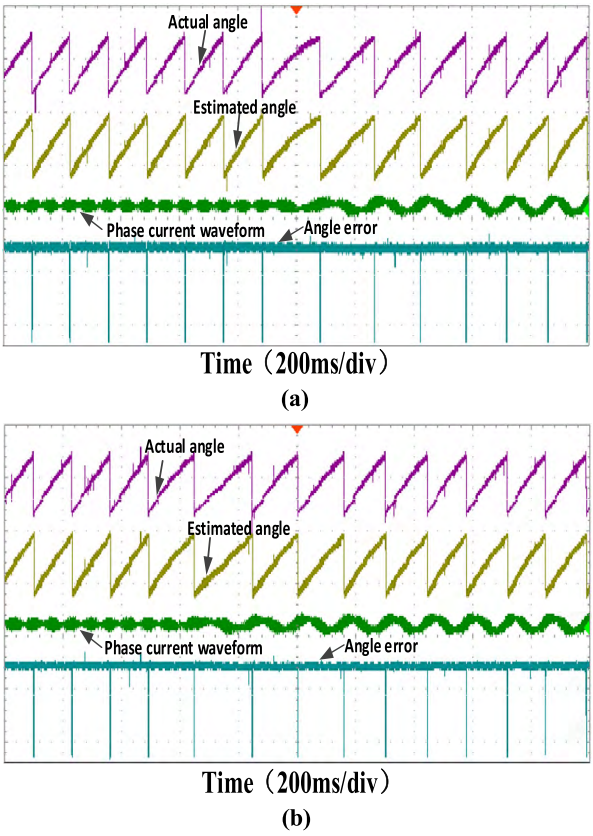

FIGURE 18. Rotor position observation under sudden load. (a) Conventional high-frequency pulsating sinusoidal voltage injection method. (b) Improved high-frequency pulsating sinusoidal voltage injection method.

D. OBSERVATION EXPERIMENT OF ROTOR POSITION OF MOTOR IN SUDDEN CHANGE OF STEERING

Fig.15 and Fig.16 respectively show the experimental waveforms of the rotor position when the motor steering abruptly changes with the conventional high-frequency pulsating sinusoidal voltage injection method and the improved high-frequency pulsating sinusoidal voltage injection method at the speed of 100rpm.

It can be seen from the experimental waveform that the two high-frequency injection methods can effectively observe the rotor position information under the condition of sudden change of the steering. The conventional high-frequency pulsating sinusoidal voltage injection method has an angular error of about 0.17 rad and a phase delay of about 0.1 rad. The improved high-frequency pulsating sinusoidal voltage injection method has an angular error of about 0.12 rad and a phase delay of about 0.06 rad. Compared with previous method, the angle observation error is smaller and the phase delay is also reduced.

E. OBSERVATION EXPERIMENT OF ROTOR POSITION OF MOTOR UNDER SUDDEN LOAD

Fig.17 is the phase current waveform of the high-frequency pulsating sinusoidal voltage injection method under sudden load, in which the amplitude of the injected sinusoidal wave is 10V and the frequency is 1000Hz.

It can be seen that the phase current of the motor using high-frequency pulsating sinusoidal voltage injection method contains high-frequency current response and has good sinusoidal degree under load.

Given the speed of 100 rpm, Fig.18 shows the experimental waveforms of rotor position observation with two high-frequency injection methods under abrupt load change. Among them, Fig.18(a) is the rotor position observation waveform for the conventional high-frequency pulsating sinusoidal voltage injection method, Fig.18(b) is the rotor position observation waveform for the improved high-frequency pulsating sinusoidal voltage injection method.

It can be seen from the experimental waveform that both high-frequency pulsating sinusoidal voltage injection methods have good resistance to load disturbance. In the case of a sudden load change, the motor will experience some jitter and will soon return to a steady state. The estimated error of the conventional high-frequency pulsating sinusoidal voltage injection method is about 0.15 rad, and the improved high-frequency pulsating sinusoidal voltage injection method has an estimation error of about 0.12 rad. The improved high-frequency pulse injection method has a smaller estimation error than the pre-improvement angle.

V. CONCLUSION

In this paper, an improved position-sensorless control method for PMSM based on high-frequency signal injection into a rotary reference frame is proposed. Firstly, in order to solve the problem that the conventional high-frequency voltage injection method is not suitable for motor with no obvious salient pole effect, a method of extracting high-frequency current response signal in α-β two-phase stationary reference frame is proposed. Then, based on the improved high-frequency pulsating sinusoidal voltage injection method, this paper adopts the method that the static two-phase current $l_{\alpha h}$ and $i_{\beta h}$ have modulated directly. Only the low-pass filter is required to obtain the signal containing the rotor position information, and the band-pass filter is omitted, which simplifies the system structure and eliminates the effects of bandpass filters on signal amplitude and phase. Finally, experiments show that the dynamic steady state performance of this method is better than the previous method.

REFERENCES

[1] R. Ni, D. Xu, G. Wang, X. Gui, G. Zhang, H. Zhan, and C. Li, "Efficiency enhancement of general AC drive system by remanufacturing induction motor with interior permanent-magnet rotor," *IEEE Trans. Ind. Electron.*, vol. 63, no. 2, pp. 808–820, Feb. 2016.

[2] G. Zhang, G. Wang, D. Xu, and N. Zhao, "ADALINE-network-based PLL for position sensorless interior permanent magnet synchronous motor drives," *IEEE Trans. Power Electron.*, vol. 31, no. 2, pp. 1450–1460, Feb. 2016.

[3] S. K. Kommuri, M. Defoort, H. R. Karimi, and K. C. Veluvolu, "A robust observer-based sensor fault-tolerant control for PMSM in electric vehicles," *IEEE Trans. Ind. Electron.*, vol. 63, no. 12, pp. 7671–7681, Dec. 2016.

[4] P. E. Kakosimos, A. G. Sarigiannidis, M. E. Beniakar, A. G. Kladas, and C. Gerada, "Induction motors versus permanent-magnet actuators for aerospace applications," *IEEE Trans. Ind. Electron.*, vol. 61, no. 8, pp. 4315–4325, Aug. 2014.

[5] R. Ni, D. Xu, G. Wang, L. Ding, G. Zhang, and L. Qu, "Maximum efficiency per ampere control of permanent-magnet synchronous machines," *IEEE Trans. Ind. Electron.*, vol. 62, no. 4, pp. 2135–2143, Apr. 2015.
[6] X. Zhang, B. Hou, and Y. Mei, "Deadbeat predictive current control of permanent-magnet synchronous motors with stator current and disturbance observer," *IEEE Trans. Power Electron.*, vol. 32, no. 5, pp. 3818–3834, May 2017.
[7] G. Xie, K. Lu, S. K. Dwivedi, J. R. Rosholm, and F. Blaabjerg, "Minimum-voltage vector injection method for sensorless control of PMSM for low-speed operations," *IEEE Trans. Power Electron.*, vol. 31, no. 2, pp. 1785–1794, Feb. 2016.
[8] S.-C. Yang, S.-M. Yang, and J.-H. Hu, "Robust initial position estimation of permanent magnet machine with low saliency ratio," *IEEE Access*, vol. 6, pp. 2685–2695, Feb. 2017.
[9] H.-Q. Nguyen and S.-M. Yang, "Rotor position sensorless control of wound-field flux-switching machine based on high frequency square-wave voltage injection," *IEEE Access*, vol. 6, pp. 48776–48784, Aug. 2018.
[10] N. K. Quang, N. T. Hieu, and Q. P. Ha, "FPGA-based sensorless PMSM speed control using reduced-order extended Kalman filters," *IEEE Trans. Ind. Electron.*, vol. 61, no. 12, pp. 6574–6582, Dec. 2014.
[11] T. Bernardes, V. F. Montagner, H. A. Gründling, and H. Pinheiro, "Discrete-time sliding mode observer for sensorless vector control of permanent magnet synchronous machine," *IEEE Trans. Ind. Electron.*, vol. 61, no. 4, pp. 1679–1691, Apr. 2014.
[12] G. Zhang, J. Yang, M. Su, W. Tang, and F. Blaabjerg, "Stator-current-based MRAS observer for the sensorless control of the brushless doubly-fed induction machine," in *Proc. IEEE Appl. Power Electron. Conf. Expo.*, Mar. 2017, pp. 3150–3155.
[13] X. Sun, L. Chen, Z. Yang, and H. Zhu, "Speed-sensorless vector control of a bearingless induction motor with artificial neural network inverse speed observer," *IEEE/ASME Trans. Mechatronics*, vol. 18, no. 4, pp. 1357–1366, Aug. 2013.
[14] X. Sun, L. Chen, H. Jiang, Z. Yang, J. Chen, and W. Zhang, "High-performance control for a bearingless permanent-magnet synchronous motor using neural network inverse scheme plus internal model controllers," *IEEE Trans. Ind. Electron.*, vol. 63, no. 6, pp. 3479–3488, Jun. 2016.
[15] F.-J. Lin, K.-J. Yang, I.-F. Sun, and J.-K. Chang, "Intelligent position control of permanent magnet synchronous motor using recurrent fuzzy neural cerebellar model articulation network," *IET Electr. Power Appl.*, vol. 9, no. 3, pp. 248–264, Oct. 2014.
[16] X. Qiu, W. Wang, J. Yang, J. Jiang, and J. Yang, "Phase-inductance-based position estimation method for interior permanent magnet synchronous motors," *Energies*, vol. 10, no. 12, p. 2002, 2017.
[17] Z. Zhu, A. Almarhoon, and P. Xu, "Improved rotor position estimation accuracy by rotating carrier signal injection utilizing zero-sequence carrier voltage for dual three-phase PMSM," *IEEE Trans. Ind. Electron.*, vol. 64, no. 6, pp. 4454–4462, Jun. 2017.
[18] T. Szalai, G. Berger, and J. Petzoldt, "Stabilizing sensorless control down to zero speed by using the high-frequency current amplitude," *IEEE Trans. Power Electron.*, vol. 29, no. 7, pp. 3646–3656, Jul. 2014.
[19] M. Seilmeier and B. Piepenbreier, "Sensorless control of PMSM for the whole speed range using two-degree-of-freedom current control and HF test current injection for low-speed range," *IEEE Trans. Power Electron.*, vol. 30, no. 8, pp. 4394–4403, Aug. 2015.
[20] Y.-D. Yoon and S.-K. Sul, "Sensorless control for induction machines based on square-wave voltage injection," *IEEE Trans. Power Electron.*, vol. 29, no. 7, pp. 3637–3645, Jul. 2014.
[21] S.-C. Yang and Y.-L. Hsu, "Full speed region sensorless drive of permanent-magnet machine combining saliency-based and back-EMF-based drive," *IEEE Trans. Ind. Electron.*, vol. 64, no. 2, pp. 1092–1101, Feb. 2017.
[22] G. Zhang, G. Wang, B. Yuan, R. Liu, and D. Xu, "Active disturbance rejection control strategy for signal injection-based sensorless IPMSM drives," *IEEE Trans. Transp. Electrific.*, vol. 4, no. 1, pp. 330–339, Mar. 2018.
[23] Z. Q. Zhu and L. M. Gong, "Investigation of effectiveness of sensorless operation in carrier-signal-injection-based sensorless-control methods," *IEEE Trans. Ind. Electron.*, vol. 58, no. 8, pp. 3431–3439, Aug. 2011.
[24] S. Kim and S.-K. Sul, "High performance position sensorless control using rotating voltage signal injection in IPMSM," in *Proc. 14th Eur. Conf. Power Electron. Appl. (EPE)*, Aug./Sep. 2011, pp. 1–10.
[25] C. M. Wolf and R. D. Lorenz, "Using the motor drive as a sensor to extract spatially dependent information for motion control applications," *IEEE Trans. Ind. Appl.*, vol. 47, no. 3, pp. 1344–1351, May/Jun. 2011.
[26] S.-C. Yang and R. D. Lorenz, "Surface permanent-magnet machine self-sensing at zero and low speeds using improved observer for position, velocity, and disturbance torque estimation," *IEEE Trans. Ind. Appl.*, vol. 48, no. 1, pp. 151–160, Jan./Feb. 2012.
[27] G. Wang, G. Zhang, R. Yang, and D. Xu, "Robust low-cost control scheme of direct-drive gearless traction machine for elevators without a weight transducer," *IEEE Trans. Ind. Appl.*, vol. 48, no. 3, pp. 996–1005, May/Jun. 2012.
[28] Y.-D. Yoon, S.-K. Sul, S. Morimoto, and K. Ide, "High-bandwidth sensorless algorithm for AC machines based on square-wave-type voltage injection," *IEEE Trans. Ind. Appl.*, vol. 47, no. 3, pp. 1361–1370, May/Jun. 2011.
[29] J. M. Liu and Z. Q. Zhu, "Novel sensorless control strategy with injection of high-frequency pulsating carrier signal into stationary reference frame," *IEEE Trans. Ind. Appl.*, vol. 50, no. 4, pp. 2574–2583, Jul./Aug. 2014.
[30] X. Qiu, W. Huang, and F. Bu, "Sensorless direct torque control of interior permanent magnet synchronous machines over wide speed range," *Trans. China Electrotech. Soc.*, vol. 29, no. 9, pp. 92–99, 2014.
[31] H. Jiabing and H. Y. Nianhong, "Sensorless technology of surface-mounted PMSM at zero speed based on magnetic saturation salient effect," *J. Elect. Eng. China*, vol. 26, no. 10, pp. 152–157, 2006.
[32] L. Ying, "Research on high-frequency pulse signal injection sensorless technology for permanent magnet synchronous motor," Nanjing Univ. Aeronaut. Astronaut., Nanjing, China, Tech. Rep., 2012.
[33] S.-I. Kim and R.-Y. Kim, "Analysis and compensation of band-pass-filter delay for a high frequency signal injected sensorless control," in *Proc. 17th EPE ECCE-Eur.*, Sep. 2015, pp. 1–8.
[34] S. Jung and J.-I. Ha, "Design and analysis of analog filtering method for signal injection based sensorless control," in *Proc. 29th APEC*, Mar. 2014, pp. 1573–1578.

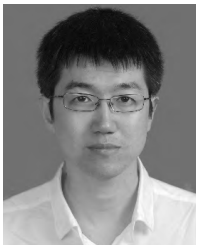

SHUANG WANG was born in Jilin, China, in 1977. He received the B.S., M.S., and Ph.D. degrees in electrical engineering from the Harbin Institute of Technology, Harbin, China, in 2000, 2005, and 2009, respectively. Since 2010, he has been with the School of Mechatronic Engineering and Automation, Shanghai University, Shanghai, China, where he is currently an Assistant Professor. His current research interests include intelligent control theory and its application to new energy vehicles, power electronics, and servo control systems.

KANG YANG received the B.S. degree in electrical engineering and automation from Anhui Jianzhu University, Hefei, China, in 2014 and 2018, respectively. He is currently pursuing the M.S. degree with the School of Mechatronic Engineering and Automation, Shanghai University, Shanghai, China. His research interests include position-sensorless control, high-frequency voltage injection control, power electronics devices, and electric motor control systems.

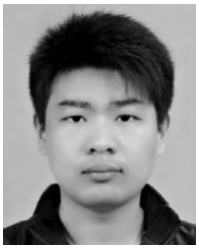

KANG CHEN was born in 1993. He received the B.E. degree from the Shandong University of Technology, Zibo, China, in 2016. He is currently pursuing the M.S. degree with the School of Mechanical Engineering and Automation, Shanghai University, Shanghai, China. His research interests include motor drives and control of PMSM.